

**Table I.** Comparison of Electrostatic Solvation Free Energies Obtained from Free Energy Perturbation (FEP) and Continuum Electrostatic (FDPB) Methods

solute <sup>a</sup>	-ΔG <sub>sol</sub> , kcal/mol	
	FEP	FDPB (ε = 1)
methanol	7.1 ± 0.3	8.09
ethanol	7.4 ± 0.2	7.84
2-propanol	7.1 ± 0.3	5.37
acetone	4.5 ± 0.2	3.89
methyl acetate	3.1 ± 0.2	2.61
acetic acid	6.8 ± 0.3	10.06
N,N-dimethylacetamide	7.5 ± 0.5	6.19
acetamide	10.8 ± 0.5	12.95
(Z)-N-methylacetamide	10.1 ± 0.5	9.77
(E)-N-methylacetamide	7.4 ± 0.6	6.19
(E)-N-methylacetamide dimer	4.6 ± 0.2	3.77
alanine dipeptide (C7eq)	13.1 ± 0.4	13.85
alanine dipeptide (C5)	12.3 ± 0.5	12.87
alanine dipeptide (αR)	20.9 ± 0.7	21.09
benzene	1.9 ± 0.3	2.19
toluene	0.7 ± 0.2	1.69
phenol	8.0 ± 0.7	8.79
ammonium ion	103.9 ± 0.7 <sup>b</sup>	95.19
acetate ion	91.3 ± 1.4 <sup>b</sup>	77.59
ammonium acetate	47.7 ± 0.9	40.5

<sup>a</sup>Geometries obtained by energy minimization using OPLS/AMBER in vacuo. <sup>b</sup>Value includes a -19.3 kcal/mol correction for the 8.5-Å solvent cutoff employed (Jorgensen, W. L.; Blake, J. F.; Buckner, J. K. *Chem. Phys.* **1989**, *129*, 193).

each solute over eight equal stages. TIP4P water is reported to have a dielectric constant of ~50<sup>11</sup> while we used the experimental value of about 80 in the FDPB calculations. Using a dielectric constant of 50 results in only minor changes in the FDPB energies. The FEP simulations followed a standard protocol in which 600 000 configurations were used for equilibration and then 10 blocks of 100 000 configurations were averaged to give the free energy change for each stage. The energies reported are the averages of the charging and discharging free energies. The error limits correspond to the root mean square of the standard deviations of the energy fluctuations of each stage.

The results are summarized in Table I and Figure 1. It is evident that, overall, there is excellent agreement between the FEP calculations and the FDPB calculations. Whether this should be viewed as confirming the continuum treatment or the TIP4P model is to some extent a matter of one's perspective. In any case, the success of the Born model of ion solvation,<sup>12</sup> which has been explained in part by a recent FEP study,<sup>13</sup> is extended here to the more general case of polyatomic solutes with complex charge distributions. It should be pointed out that the FDPB calculations produce solvation free energies for the ammonium and acetate ions which are closer to the experimental values than those obtained from the free energy simulations (only the sum of the experimental values can be reliably determined experimentally; for ammonium and acetate the value is ~15 kcal/mol<sup>14</sup>). The tendency of current water models to overestimate the solvation free energies of ions is well-known and appears due, at least in part, to the neglect of electronic polarization.<sup>13,15</sup>

The agreement between the two sets of calculations which ignore electronic polarizability suggests that there are now available two very different methods which yield a consistent picture of the electrostatic component of solute-solvent interactions. The FDPB calculations are extremely fast (about 10 s on a Convex C2 computer) but at the sacrifice of information as to the organization of solvent molecules around the solute. The FEP calculations require 3–4 orders of magnitude more computer time but can

provide a detailed description of solvent structure when that is of interest. Finally, it should be pointed out that no attempt has been made to optimize parameters for the FDPB calculations. The OPLS parameters were used so as to facilitate comparison with the FEP calculations and might ultimately have to be modified in future attempts to reproduce experimental solvation energies.<sup>16</sup>

**Supplementary Material Available:** Nonbonded parameters and partial charge sets for the molecules listed in Table I (10 pages). Ordering information is given on any current masthead page.

(16) Supported by NIH Grant GM-30518 (B.H.) and NSF Grant CHE89 11008 (W.C.S.).

### Group 4 Metal Dicarbolide Chemistry. Synthesis, Structure, and Reactivity of Electrophilic Alkyl Complexes (Cp\*)(C<sub>2</sub>B<sub>9</sub>H<sub>11</sub>)M(R) (M = Hf, Zr)

Donna J. Crowther, Norman C. Baenziger, and Richard F. Jordan\*

Department of Chemistry, University of Iowa  
Iowa City, Iowa 52242

Received October 29, 1990

Fourteen-electron, d<sup>0</sup> bent-metallocene alkyl complexes of general type (C<sub>5</sub>R<sub>5</sub>)<sub>2</sub>M(R)<sup>++</sup> exhibit a rich insertion, olefin polymerization, and C–H activation chemistry which is highly sensitive to the structural and electronic properties of the (C<sub>5</sub>R<sub>5</sub>)<sub>2</sub>M fragment.<sup>1–4</sup> Known complexes of this type include *neutral* group 3<sup>1</sup> and lanthanide<sup>2</sup> complexes (C<sub>5</sub>R<sub>5</sub>)<sub>2</sub>M(R) and *cationic* group 4<sup>3</sup> and actinide<sup>4</sup> species (C<sub>5</sub>R<sub>5</sub>)<sub>2</sub>M(R)<sup>+</sup>. Here we describe a new class of *neutral, d<sup>0</sup>, group 4 metal bent-metallocene* complexes of general form (Cp\*)(C<sub>2</sub>B<sub>9</sub>H<sub>11</sub>)M(R) (M = Zr, Hf). The formal replacement of a uninegative C<sub>5</sub>R<sub>5</sub><sup>-</sup> ligand of (C<sub>5</sub>R<sub>5</sub>)<sub>2</sub>M(R)<sup>+</sup> by the isolobal, dinegative dicarbolide ligand (C<sub>2</sub>B<sub>9</sub>H<sub>11</sub>)<sup>2-</sup><sup>5</sup> reduces the overall charge by 1 unit but leaves the gross structural and metal frontier orbital properties unchanged, thus allowing preparation of electrophilic metal alkyl complexes with new metal/charge combinations.

Hawthorne has developed the coordination chemistry of C<sub>2</sub>B<sub>9</sub>H<sub>11</sub><sup>2-</sup>, which is electronically and sterically comparable to Cp\*<sup>-</sup>.<sup>5</sup> The parent acid C<sub>2</sub>B<sub>9</sub>H<sub>13</sub> contains two acidic hydrogens which can cleave M–C bonds of electrophilic metals.<sup>3b,5d</sup> The reaction of equimolar amounts of C<sub>2</sub>B<sub>9</sub>H<sub>13</sub><sup>6</sup> and Cp\*M(Me)<sub>3</sub> (M

(1) (a) Burger, B. J.; Thompson, M. E.; Cotter, W. D.; Bercaw, J. E. *J. Am. Chem. Soc.* **1990**, *112*, 1566. (b) Thompson, M. E.; Baxter, S. M.; Bulls, A. R.; Burger, B. J.; Nolan, M. C.; Santarsiero, B. D.; Schaefer, W. P.; Bercaw, J. E. *J. Am. Chem. Soc.* **1987**, *109*, 203. (c) den Haan, K. H.; Wielstra, Y.; Teuben, J. H. *Organometallics* **1987**, *6*, 2053. (d) Evans, W. J.; Dominguez, R.; Hanusa, T. P. *Organometallics* **1986**, *5*, 263.

(2) (a) Watson, P. L.; Parshall, G. W. *Acc. Chem. Res.* **1985**, *18*, 51. (b) Jeske, G.; Lauke, H.; Mauermann, H.; Sweptson, P. N.; Schumann, H.; Marks, T. J. *J. Am. Chem. Soc.* **1985**, *107*, 8091. (c) Evans, W. J.; Chamberlain, L. R.; Ulibarri, T. A.; Ziller, J. *J. Am. Chem. Soc.* **1988**, *110*, 6423. (d) Heeres, H. J.; Meetsma, A.; Teuben, J. H. *Angew. Chem., Int. Ed. Engl.* **1990**, *29*, 420. (e) Gagne, M. R.; Marks, T. J. *J. Am. Chem. Soc.* **1989**, *111*, 4108.

(3) (a) Eisch, J. J.; Piotrowski, A. M.; Brownstein, S. K.; Gabe, E. J.; Lee, F. L. *J. Am. Chem. Soc.* **1985**, *107*, 7219. (b) Hlatky, G. G.; Turner, H. W.; Eckmann, R. R. *J. Am. Chem. Soc.* **1989**, *111*, 2728. (c) Jordan, R. F.; Bajgur, C. S.; Willet, R.; Scott, B. J. *J. Am. Chem. Soc.* **1986**, *108*, 7410. (d) Jordan, R. F.; LaPointe, R. E.; Bajgur, C. S.; Echols, S. F.; Willet, R. J. *J. Am. Chem. Soc.* **1987**, *109*, 4111. (e) Christ, C. S.; Eyley, J. R.; Richardson, D. E. *J. Am. Chem. Soc.* **1990**, *112*, 596. (f) Bockmann, M.; Jagger, A. J.; Nicholls, J. C. *Angew. Chem., Int. Ed. Engl.* **1990**, *29*, 780.

(4) Lin, Z.; LeMarechal, J.-F.; Sabat, M.; Marks, T. J. *J. Am. Chem. Soc.* **1987**, *109*, 4127.

(5) (a) Hawthorne, M. F. *Acc. Chem. Res.* **1968**, *1*, 281. (b) Salentine, C. G.; Hawthorne, M. F. *Inorg. Chem.* **1976**, *15*, 2872. (c) Fronczek, F. R.; Halstead, G. W.; Raymond, K. N. *J. Am. Chem. Soc.* **1977**, *99*, 1769. (d) Schubert, D. M.; Bandman, M. A.; Rees, W. S., Jr.; Knobler, C. B.; Lu, P.; Nam, W.; Hawthorne, M. F. *Organometallics* **1990**, *9*, 2046. (e) Manning, M. J.; Knobler, C. B.; Hawthorne, M. F. *J. Am. Chem. Soc.* **1988**, *110*, 4458. (f) Hanusa, T. P. *Polyhedron* **1982**, *1*, 661.

(6) Wiesboeck, R. A.; Hawthorne, M. F. *J. Am. Chem. Soc.* **1964**, *86*, 1642.

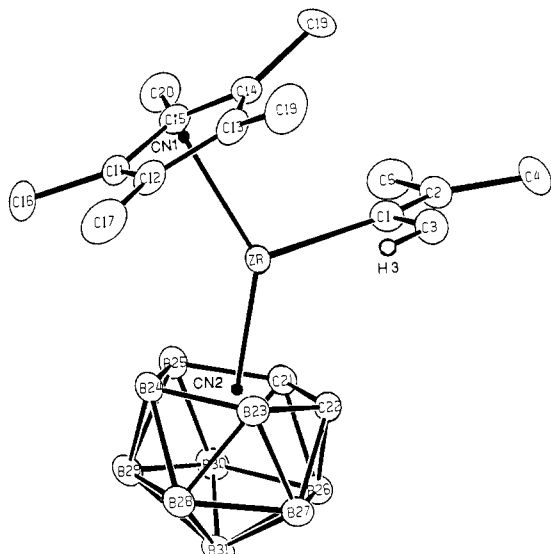
(11) Neumann, M. *J. Chem. Phys.* **1986**, *85*, 1567.

(12) Rashin, A.; Honig, B. *J. Phys. Chem.* **1985**, *89*, 5588.

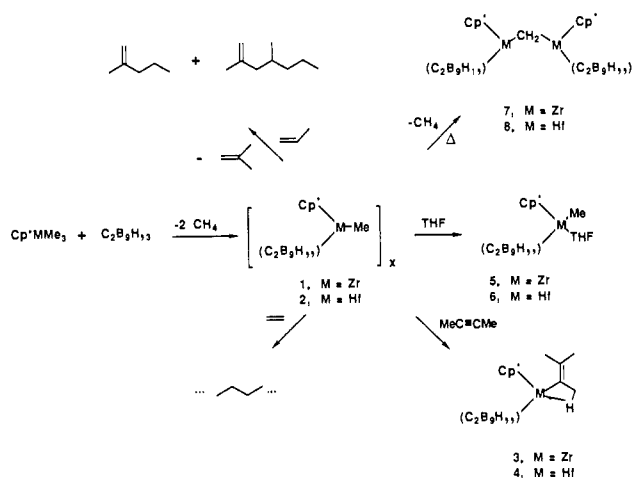
(13) Jayaram, B.; Fine, R.; Sharp, K.; Honig, B. *J. Phys. Chem.* **1989**, *93*, 4320.

(14) Honig, B.; Hubbell, W. *Proc. Nat. Acad. Sci. U.S.A.* **1984**, *81*, 5412.

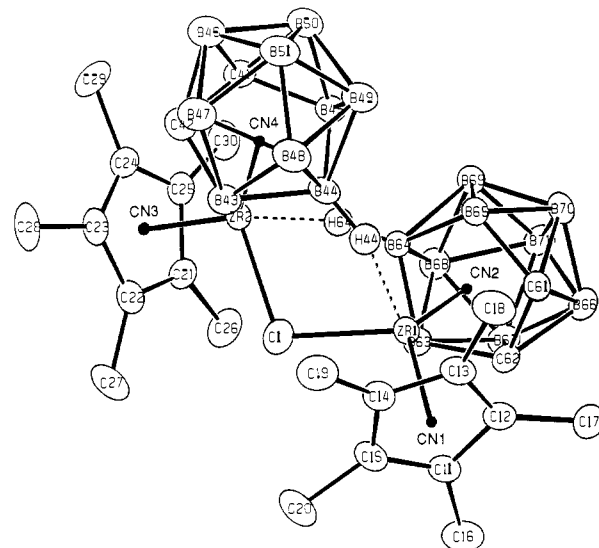
(15) Chandrasekhar, J.; Spellmeyer, D. C.; Jorgensen, W. L. *J. Am. Chem. Soc.* **1984**, *106*, 903.

Figure 1. X-ray structure of  $(\text{Cp}^*)(\text{C}_2\text{B}_9\text{H}_{11})\text{Zr}[\text{C}(\text{Me})=\text{CMe}_2]$  (**3**).

## Scheme I



= Zr,<sup>7</sup> Hf<sup>8</sup>) in aromatic solvent (23 °C, 2 h for Zr, 24 h for Hf) yields  $[(\text{Cp}^*)(\text{C}_2\text{B}_9\text{H}_{11})\text{M}(\text{Me})]_x$  (**1**, M = Zr, 95%; **2**, M = Hf, 87%; Scheme I).<sup>9</sup> Solution molecular weight measurements for **2** are inconclusive to date due to the limited solubility and high reactivity of this compound, and **1** is insoluble in hydrocarbons. However, both **1** and **2** react with 2-butyne via single insertion (benzene, 23 °C, <5 min) to yield the monomeric alkenyl complexes  $(\text{Cp}^*)(\text{C}_2\text{B}_9\text{H}_{11})\text{M}[\text{C}(\text{Me})=\text{CMe}_2]$  (**3**, M = Zr, 56%; **4**, M = Hf, 71%, Scheme I). An X-ray analysis of **3** (Figure 1) clearly establishes the presence of an  $\eta^5\text{-C}_2\text{B}_9\text{H}_{11}^{2-}$  ligand and a bent-metallocene geometry at Zr (centroid–Zr–centroid angle 141.3°) similar to that in  $(\text{C}_5\text{R}_5)_2\text{M}(\text{R})^{m+}$  complexes.<sup>10,11</sup> The Zr–( $\text{C}_2\text{B}_9\text{H}_{11}$ -centroid) distance (2.045 Å) is ca. 0.15 Å shorter than the Zr–( $\text{Cp}^*$ -centroid) distance (2.196 Å), as expected on the basis of charge and steric considerations, and the latter distance

Figure 2. X-ray structure of  $[(\text{Cp}^*)(\text{C}_2\text{B}_9\text{H}_{11})\text{Zr}]_2(\mu\text{-CH}_2)$  (**7**).

is normal for  $\text{Cp}^*\text{Zr}(\text{IV})$  complexes.<sup>11</sup> The alkenyl group lies in the plane between the two  $\eta^5$  ligands and is distorted by an agostic interaction involving one of the  $\beta\text{-CH}_3$  hydrogens (Zr–H3C, 2.29 Å; Zr–C3, 2.702 (4) Å) which results in distorted angles at C1 (Zr–C1–C2, 147.8 (4)°; Zr–C1–C3, 91.17 (25)°).<sup>12</sup> Complexes **3** and **4** do not undergo further insertion chemistry with 2-butyne, and **3** does not coordinate THF. Complexes **1** and **2** form THF adducts  $(\text{Cp}^*)(\text{C}_2\text{B}_9\text{H}_{11})\text{M}(\text{Me})(\text{THF})$  (**5**, M = Zr; **6**, M = Hf) which do not undergo exchange with free THF on the NMR time scale at 23 °C. However, **5** reacts readily with 2-butyne to yield **3**.

Complexes **1** and **2** are moderately active ethylene polymerization catalysts (**1**: (1.2 g of PE)/(mmol of Zr-atm·min); hexane, 20 °C, 150 psi). Complexes **1** and **2** also catalyze the oligomerization of propylene to 2-methylpentene (70%, **1**; 85%, **2**) and 2,4-dimethylheptene (25%, **1**; 10%, **2**) as major products (**1**: >1 t.o./min, toluene, 25 °C, <1 atm). Isobutene was detected as a minor product by GC. This product distribution is characteristic of an insertion/ $\beta\text{-H}$  elimination process.

Thermolysis of **1** in toluene-*d*<sub>8</sub> (45 °C, 2 h) quantitatively yields the novel methylidene-bridged complex  $[(\text{Cp}^*)(\text{C}_2\text{B}_9\text{H}_{11})\text{Zr}]_2(\mu\text{-CH}_2)$  (**7**) and  $\text{CH}_4$ .<sup>13</sup> The structure of **7** was determined by X-ray analysis (Figure 2) and consists of two bent-metallocene Zr centers linked by the  $\mu\text{-CH}_2$  group.<sup>14</sup> The centroid–Zr–centroid angles are smaller (average, 134.9°), and the Zr–centroid distances are slightly longer (Zr– $\text{Cp}^*$  average, 2.234 Å; Zr– $\text{C}_2\text{B}_9\text{H}_{11}$  average, 2.091 Å) than the corresponding values in **3** as a result of increased steric crowding. The staggered orientation of the two  $(\text{Cp}^*)(\text{C}_2\text{B}_9\text{H}_{11})\text{Zr}$  centers (dihedral angle between centroid–Zr–centroid planes, 71.7°) minimizes steric interactions. There are close B–H–Zr contacts involving a B–H bond of each dicarbollide ligand and the Zr to which it is not  $\eta^5$ -bonded (Zr1–H44, Zr2–H64, 2.09 Å).<sup>15</sup> Hafnium complex **2** undergoes a slower  $\text{CH}_4$  elimination reaction (75 °C, 2 days) to yield  $[(\text{Cp}^*)(\text{C}_2\text{B}_9\text{H}_{11})\text{Hf}]_2(\mu\text{-CH}_2)$  (**8**, 80% NMR).<sup>16</sup>

(7) Wolczanski, P. T.; Bercaw, J. E. *Organometallics* **1982**, *1*, 793.(8) Prepared from  $\text{Cp}^*\text{HfCl}_3$ . Roddick, D. M.; Fryzuk, M. D.; Seidler, G. L.; Hillhouse, G. L.; Bercaw, J. E. *Organometallics* **1985**, *4*, 97 and references therein.(9) Characterization data for **1–8** are given in the supplementary material.(10) Crystallographic data for **3** (295 K):  $a = 8.846$  (3) Å,  $b = 9.322$  (4) Å,  $c = 14.723$  (6) Å,  $\alpha = 78.45$  (4)°,  $\beta = 89.72$  (3)°,  $\gamma = 79.92$  (4)°,  $V = 1141$  (1) Å<sup>3</sup>,  $Z = 2$ , space group  $P1$ ;  $R_F = 0.040$ ,  $R_{wF} = 0.059$  for 3229 unique reflections with  $I > 3\sigma(I)$ . Other distances (Å): Zr–C1, 2.198 (4); C1–C2, 1.295 (6); C1–C3, 1.527 (6); C2–C4, 1.496 (6); C2–C5, 1.534 (7) Å.(11) For example, see ref 3b and see: (a) Bortolin, R.; Patel, V.; Munday, I.; Taylor, N. J.; Carty, A. J. *J. Chem. Soc., Chem. Commun.* **1985**, 456. (b) Young, S. J.; Olmstead, M. M.; Knudsen, M. J.; Schore, N. E. *Organometallics* **1985**, *4*, 1432. (c) Wolczanski, P. T.; Threlkel, R. S.; Santarsiero, B. D. *Acta Crystallogr., Sect. C: Cryst. Struct. Commun.* **1983**, *39C*, 1330.(12) (a) Jordan, R. F.; LaPointe, R. E.; Bradley, P. K.; Baenziger, N. C. *Organometallics* **1989**, *8*, 289. (b) Hyla-Kryspin, I.; Gleiter, R.; Kruger, C.; Zwteller, R.; Erker, G. *Organometallics* **1990**, *9*, 517.(13) For a related early metal  $\mu\text{-CR}_2$  complex, see: Smith, G. M.; Sabat, M.; Marks, T. J. *J. Am. Chem. Soc.* **1987**, *109*, 1854.(14) Crystallographic data for **7** (295 K):  $a = 15.582$  (3) Å,  $b = 17.671$  (4) Å,  $c = 17.658$  (3) Å,  $\beta = 118.42$  (2)°,  $V = 4276$  (3) Å<sup>3</sup>,  $Z = 4$ , space group  $P2_1/n$ ;  $R_F = 0.037$ ,  $R_{wF} = 0.058$  for 3414 unique reflections with  $I > 3\sigma(I)$ . Other distances (Å): Zr1–C1, 2.187 (6); Zr2–C1, 2.176 (7); Zr1–B44, 2.993 (8); Zr2–B64, 2.987 (7).(15) Similar Rh $\cdots$ H–B interactions are present in dimeric Rh dicarbollide complexes. Behnken, P. E.; Marder, T. B.; Baker, R. T.; Knobler, C. B.; Thompson, M. R.; Hawthorne, M. F. *J. Am. Chem. Soc.* **1985**, *107*, 932.(16) Labeling experiments imply a mechanism involving irreversible abstraction of a  $\text{Cp}^*$  hydrogen by  $\text{Hf-CH}_3$  to yield  $\text{CH}_4$  and an  $\eta^1, \eta^2\text{-C}_2\text{Me}_2\text{CH}_2$  "tuck-in" intermediate, followed by reaction with a  $\text{Hf-CH}_3$  C–H bond.

Our results establish that 14-electron,  $d^0$ , mixed-ring bent-metalocene complexes of general type  $(Cp^*)(C_2B_9H_{11})M(R)$  are accessible by reaction of group 4 alkyls with  $C_2B_9H_{13}$  and are structurally and electronically similar to  $d^0 (C_5R_5)_2M(R)$  and  $(C_5R_5)_2M(R)^+$  species.<sup>1-4</sup> The observation of strong ligand binding by **1** and **2** and agostic  $Zr \cdots H-C$  and  $Zr \cdots H-B$  interactions in **3** and **7** indicates that these complexes are highly electrophilic. This feature is reflected in the high olefin and acetylene insertion reactivity and in the facile reactions leading to  $\mu-CH_2$  complexes **7** and **8**.

Recent studies establish that 14-electron cationic  $Cp_2Zr(R)^+$  species exhibit enhanced insertion reactivity vs 16-electron neutral  $Cp_2Zr(R)(X)$  complexes.<sup>3</sup> The high insertion reactivity reported here for neutral **1**, **2**, and **5** and the high reactivity of neutral  $d^0 (C_5R_5)_2M(R)$  complexes<sup>1,2</sup> suggest that this difference results largely from the increased unsaturation of  $Cp_2Zr(R)^+$  rather than the charge.

**Acknowledgment.** This work was supported by DOE Grant DE-FG01-88ER13935 and NSF Grant CHE-8816445. Helpful conversations with G. G. Hlatky and A. R. Siedle are appreciated. R.F.J. gratefully acknowledges a Sloan Foundation Research Fellowship (1989-1991) and Union Carbide Research Innovation Awards (1989, 1990).

**Supplementary Material Available:** Synthetic procedures and characterization data for new compounds and details of the X-ray structure determinations of **3** and **7** (34 pages); listing of observed and calculated structure factors for **3** and **7** (24 pages). Ordering information is given on any current masthead page.

### Sequence-Specific Bifunctional DNA Ligands Based on Triple-Helix-Forming Oligonucleotides Inhibit Restriction Enzyme Cleavage under Physiological Conditions

David A. Collier,\*<sup>§</sup> N. T. Thuong,<sup>†</sup> and Claude Hélène\*<sup>†</sup>

Laboratoire de Biophysique  
Museum National d'Histoire Naturelle  
INSERM U 201, CNRS UA 481  
43 Rue Cuvier, 75005 Paris, France  
Centre de Biophysique Moléculaire  
CNRS, 45071 Orleans Cedex 02, France

Received July 13, 1990

Intermolecular triplex formation has been demonstrated to inhibit DNA-protein interactions by the observation that selective binding of a third strand of DNA at the recognition site of restriction/modification enzymes prevents cleavage or methylation of the duplex.<sup>1-3</sup> Triplex formation has the potential to precisely modulate gene expression if targeted at protein binding sites involved in the regulation of a specific gene.

Intermolecular triplex formation occurs by binding of a homopyrimidine oligonucleotide to the major groove of a homopurine-homopyrimidine stretch of DNA, parallel to the purine strand. Sequence specificity results from Hoogsteen pairing between thymine and protonated cytosine in the third pyrimidine strand and the Watson-Crick A·T and G·C pairs of the duplex, respectively.<sup>4-8</sup>

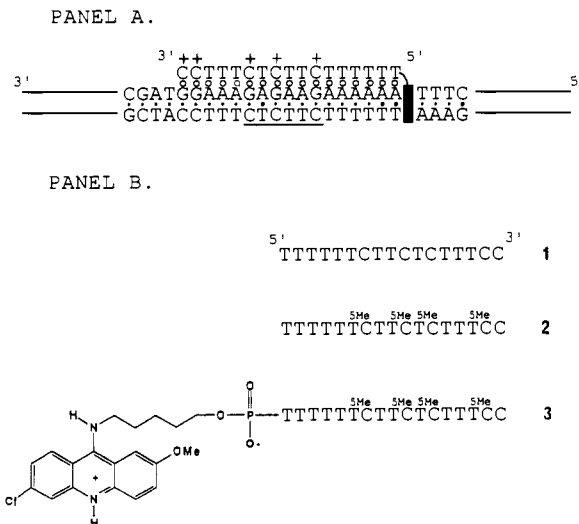


**Figure 1.** Panel A: Structure and sequence of the triple helix with the covalently attached acridine intercalated at the 5' triplex-duplex junction, showing the recognition sequence (underlined) of *Ksp632 I*. Filled dots and open circles between bases indicate Watson-Crick and Hoogsteen pairing, respectively. Protonated cytosines are indicated by the + symbol. Panel B: Structures of the oligonucleotides used for triple-helix formation. The unmodified oligonucleotide (**1**) and the oligonucleotide containing 5-methylcytosine (**2**) were synthesized by using phosphoramidite chemistry on a Pharmacia automated DNA synthesizer. The oligonucleotide with an acridine covalently attached to the 5' end (**3**) was prepared by solid-phase synthesis using the phosphoramidite derivative of 2-methoxy-6-chloro-9-[( $\omega$ -hydroxypentyl)amino]acridine as described.<sup>12</sup> Bases which are 5-methylcytosine are indicated 5Me. All oligonucleotides are parallel to the purine strand of the duplex.

**Table I.** Concentrations of Oligonucleotides Required for 50% Inhibition of Restriction Endonuclease Cleavage by *Ksp632 I* via Triple-Helix Formation<sup>a</sup>

oligonucleotide	concn required for 50% inhibn of cleavage, $\mu M$		$T_m$ of triplex-to-duplex transition at pH 7.0, $^{\circ}C$
	pH 7.0	pH 7.7	
<b>1</b> , native	4.4	>50	15 $\pm$ 0.5
<b>2</b> , 5-methylcytosine	0.85	36	22 $\pm$ 3
<b>3</b> , 5-methylcytosine/acridine	0.15	7.5	35 $\pm$ 1

<sup>a</sup>  $T_m$  measurements were performed as previously described<sup>11</sup> in 50 mM sodium cacodylate buffer (pH 7.0) by using a Kontron Uvikon 820 spectrophotometer.

The concentrations of the third strand required for specific inhibition of restriction enzyme cleavage via triple-helix formation are in the micromolar range,<sup>1,2</sup> and triplex formation and hence inhibition are dependent on low pH.<sup>1,2</sup> In order to use intermolecular triplex formation as a tool to modulate gene expression in vivo, conditions must be established whereby triplex formation is stable under physiological conditions of pH and at a concentration of the third strand that can be realistically attained in the nucleus of living cells.

In this study we have attempted to optimize the concentrations of oligodeoxynucleotides required for site-specific inhibition of protein binding to DNA by the replacement of cytosine with 5-methylcytosine and by attachment of an acridine residue to the

(4) Le Doan, T.; Perrouault, L.; Praseuth, D.; Habboub, N.; Decout, J. L.; Thuong, N. T.; Lhomme, J.; Hélène, C. *Nucleic Acids Res.* **1987**, *15*, 7749-7760.

(5) Moser, H. E.; Dervan, P. B. *Science* **1987**, *238*, 645-650.

(6) Praseuth, D.; Perrouault, L.; Le Doan, T.; Chassignol, M.; Thuong, N. T.; Hélène, C. *Proc. Natl. Acad. Sci. U.S.A.* **1988**, *85*, 1349-1353.

(7) Lyamichev, V. I.; Mirkin, S. M.; Frank-Kamenetskii, M. D.; Cantor, C. R. *Nucleic Acids Res.* **1988**, *16*, 2165-2178.

(8) Francois, J.-C.; Saison-Behmoras, T.; Hélène, C. *Nucleic Acids Res.* **1988**, *16*, 11431-11440.

(9) Bolton, B. J.; Schmitz, G. G.; Jarsch, M.; Conner, M. J.; Kessler, C. *Gene* **1988**, *66*, 31-43.

<sup>†</sup> Laboratoire de Biophysique, Museum National d'Histoire Naturelle.

<sup>§</sup> Present address: Division of Genetics, Institute of Psychiatry, Denmark Hill, London SE5 8AF, UK.

(1) Francois, J.-C.; Saison-Behmoras, T.; Thuong, N. T.; Hélène, C. *Biochemistry* **1989**, *28*, 9617-9619.

(2) Maher, J. L.; Wold, B.; Dervan, P. B. *Science* **1989**, *245*, 725-730.

(3) Hanvey, J. C.; Shimizu, M.; Wells, R. D. *Nucleic Acids Res.* **1990**, *18*, 157-161.